Mössbauer study of a glassy ferromagnet: $Fe_{40}Ni_{40}P_{14}B_6$†

C. L. Chien
Department of Physics, The Johns Hopkins University, Baltimore, Maryland 21218

R. Hasegawa
Materials Research Center, Allied Chemical Corporation, Morristown, New Jersey 07960

(Received 18 May 1977)

The glassy ferromagnet $Fe_{40}Ni_{40}P_{14}B_6$ has been studied by Mössbauer spectroscopy from 4.2 to 1000 K. In the glassy state, the average hyperfine field $H_{\text{eff}}(T)$ decreases with temperature more rapidly than that of crystalline ferromagnets due to a distribution of exchange interactions. At $T \lesssim \frac{1}{2} T_C$, $H_{\text{eff}}(T)$ has a temperature dependence of $H_{\text{eff}}(0)\,[1 - B_{3/2}(T/T_C)^{3/2} \cdots]$, indicative of spin-wave excitations. The value of $B_{3/2} = 0.47 \pm 0.07$ is four times larger than those of crystalline Fe and Ni. The Curie temperature $T_C = 537$ K is found to be well defined. At T close of T_C, $H_{\text{eff}}(T)$ behaves as a power law with a critical exponent of $\beta = 0.32 \pm 0.05$. In the glassy state and at $T > T_C$, the quadrupole spectra show asymmetrical doublets, suggesting that the electronic state of Fe may not be unique. A crystallization temperature (T_{cr}) of 700 K has been determined under high heating rate. At much lower heating rate, crystallization occurs at 670 K. The crystallized sample of $Fe_{40}Ni_{40}P_{14}B_6$ contains two ferromagnetic crystalline phases of $Fe_{55}Ni_{45}$ ($T_C = 750$ K) and $(Fe\text{-}Ni)_{30}P_7B_3$ ($T_C = 425$ K).

I. INTRODUCTION

Magnetic metallic glasses present opportunities for studying the effects of structural disorder on the properties of solids. These glassy solids have already exhibited a rich variety of phenomena in their solid-state properties in general and magnetic properties, in particular.[1] Even though these metallic glasses have no long-range order (translational symmetry), many of them exhibit ferromagnetic ordering as well as other types of more complicated magnetic orderings. Because of the special ways in which these glassy solids are synthesized, the atomic arrangements are disordered. The model of random packing of hard spheres has been shown to be a useful approximation in describing the disordered atomic arrangements in metallic glasses, although short-range order may exist in many of them.[2] As a result of the disordered atomic arrangements, many quantities which are well defined in crystalline solids have a distribution of values such as magnetic moments, exchange interaction, hyperfine field, electric field gradient, etc. Consequently, some properties of the glassy metallic solids may be similar to those of crystalline solids, while other properties are markedly different.

The glassy state of metallic glasses is not a thermodynamic equilibrium state, i.e., it is a metastable state, and exists only at sufficiently low temperatures. At high enough temperatures, the glassy state unavoidably and irreversibly transforms into the crystalline state. The crystallization process and the behavior of the subsequent crystalline phases may shed light on the stability and the properties of the glassy state.

In this work, a detailed study of a glassy ferromagnet $Fe_{40}Ni_{40}P_{14}B_6$ (Metglas® 2826)[3] has been made by Mössbauer spectroscopy from 4.2 to 1000 K. The magnetic properties and the hyperfine interactions of $Fe_{40}Ni_{40}P_{14}B_6$ in its glassy state, the glass-to-crystalline transition and the behavior of the crystalline phases have been studied.

II. EXPERIMENTAL

Samples of glassy $Fe_{40}Ni_{40}P_{14}B_6$ were made by the technique of rapid quenching from the melt. The material is in long ribbon form with a nominal width of 3 mm and thickness of 35 μm. The noncrystalline nature of the sample was checked by x rays. All absorbers were made by placing a few ribbons parallel to each other and covering an area of about 1.5×1.5 cm. For measurements at T less than 300 K, these ribbons were usually sandwiched between thin Al foils and held together by vacuum grease. The Al foils were clamped to the oxygen-free high-conductivity copper cold foot. For measurements at T greater than 300 K, the ends of the ribbons were cemented to a thin piece of synthetic mica.

For measurements at T less than 300 K, a continuous-flow cryostat in conjunction with proportional heating was used to maintain the sample temperature with stability better than 0.2 K. The temperature of the sample was monitored by a precision Pt resistor. For measurement at 4.2 K, the sample was immersed in the liquid He

bath. For measurements at T greater than 300 K, heating took place in vacuum of 10^{-5} Torr. The sample temperature, with stability better than 1 K during the measurement, was measured via a thermocouple.

A conventional spectrometer in constant acceleration mode was used with a radioactive source of ^{57}Co in either Cr or Rh. The majority of the measurements were performed using the standard transmission geometry, in which the γ ray was perpendicular to the sample plane. In some cases, the sample plane was at an angle other than 90° with respect to the γ ray so that additional information about the magnetization axis could be obtained. We have also used the method of frequency counting at a fixed Doppler velocity to detect the magnetic ordering temperatures.

III. RESULTS AND DISCUSSIONS

A. Magnetic hyperfine interaction

Spectra of $Fe_{40}Ni_{40}P_{14}B_6$ measured at 300 K are shown in Fig. 1. It is clear from the broad line widths that these spectra do not represent a unique hyperfine magnetic field. This is expected from the noncrystalline nature of the sample, in which there are many inequivalent Fe sites. The measured spectrum is the consequence of a distribution of hyperfine fields. However, the hyperfine field distribution is reasonably narrow so that the spectral lines remain well defined. We have used two methods to analyze these spectra in order to obtain the mean hyperfine field value and its temperature dependence. From the well-defined positions of the six lines, one obtains $H_{\rm eff}(T)$, the average hyperfine field at temperature T. We have also analyzed these spectra by assuming an asymmetrical Gaussian hyperfine field distribution[4] about a peak value $H_e(T)$. Good fits, as demonstrated by the solid curves in all of these spectra, can be obtained by either method. The determined values of $H_{\rm eff}(T)$ and $H_e(T)$ are slightly and consistently different by about 2%. However, in reduced units, the values of $H_{\rm eff}(T)/H_{\rm eff}(0)$ and $H_e(T)/H_e(0)$ are virtually the same. Therefore, although the values of the mean hyperfine field are slightly model dependent, the values of the reduced hyperfine field are essentially not.

From the noncrystalline nature of the sample, the Fe site symmetry in general will not be cubic. Therefore, in addition to the magnetic hyperfine interaction, there is also a quadrupole interaction due to the nonzero electric field gradients (EFG). But as shown in Fig. 1(a), there is little apparent quadrupole interaction, since the line positions are very symmetrical. This can be explained as follows. The quadrupole interaction at each site can be approximately described by $e^2qQ(3\cos^2\theta' - 1)$, where e^2qQ is the quadrupole interaction energy and θ' is the angle between the z axis of the principal (EFG) tensors and the hyperfine field. The z axis of the EFG is determined by the site symmetry, which varies spatially throughout the sample. On the other hand, the magnetic hyperfine field, which is antiparallel to the magnetization axis in a ferromagnetic sample does not vary randomly. A collective measurement of a macroscopic sample, in effect, takes the spatial average of $(3\cos^2\theta' - 1)$, which yields zero. Quadrupole effect in noncrystalline magnetic solids can be unequivocally measured only in the paramagnetic state ($T > T_C$), in which the magnetic interaction is "turned off."

B. Magnetization axis

It is well known that the ^{57}Fe magnetic hyperfine pattern consists of six lines with intensity ratio of $3{:}b{:}1{:}1{:}b{:}3$, where $b = 4\sin^2\theta/(1+\cos^2\theta)$ and θ is the angle between the magnetization axis and the γ-ray direction.[5] The values of b vary from 0 to 4 for $\theta = 0°$–$90°$. For a sample containing more than one magnetization direction, the value of b has to be averaged accordingly. The measured spectrum therefore supplies information concerning the direction of magnetization. Since it is measured microscopically and without the requirement of an external magnetic field, it is useful in the case of transition metal based glassy ferromagnets in which the anisotropy and the coercivity are generally very small.[1]

For a glassy sample, since the six lines do not have the same linewidth, due to a hyperfine field distribution, one compares area ratios rather than intensity ratios. Figure 1 shows three spectra at 300 K with different geometries of measurements which are shown on the right. Long and short rectangles represent the long and the short edges of a ribbon, and the wavy line denotes the γ-ray direction. Figure 1(a) shows the spectrum taken with the γ ray perpendicular to the ribbon plane. From the area ratio of about 3:4:1, one immediately concludes that the magnetization axis is in the ribbon plane. There are two further possibilities: random easy axis in the ribbon plane, or a preferred direction in the ribbon plane. To distinguish these two cases, we rotated the ribbon plane by about 30° with respect to the γ ray while keeping either the long edge [Fig. 1(b)] or the short edge [Fig. 1(c)] perpendicular to the γ ray. The spectrum shown in Fig. 1(b) is practically the same as that shown in Fig. 1(a), whereas the spectrum shown in Fig. 1(c) is considerably different in No. 2 and 5 peaks. These results are possible

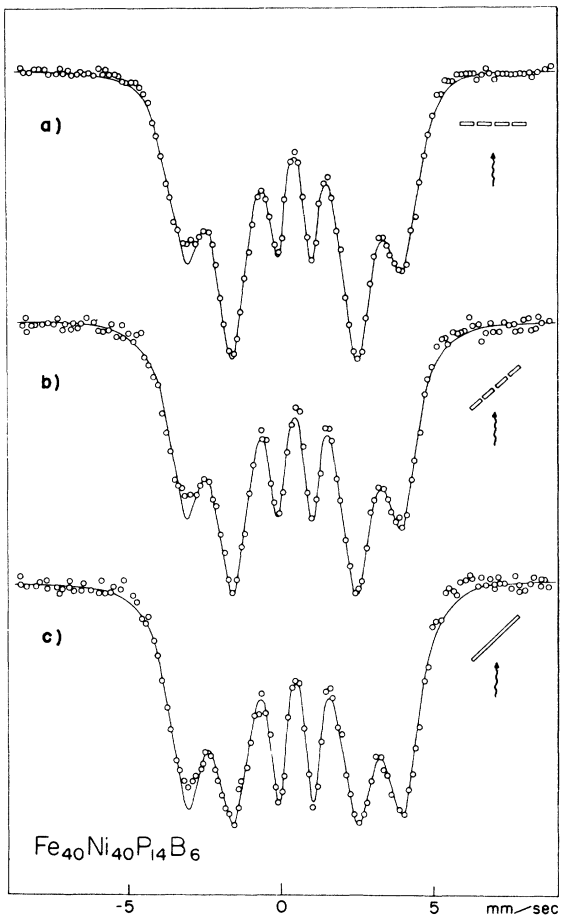

FIG. 1. Mössbauer spectra of $Fe_{40}Ni_{40}P_{14}B_6$ at 300 K under different geometries (see text).

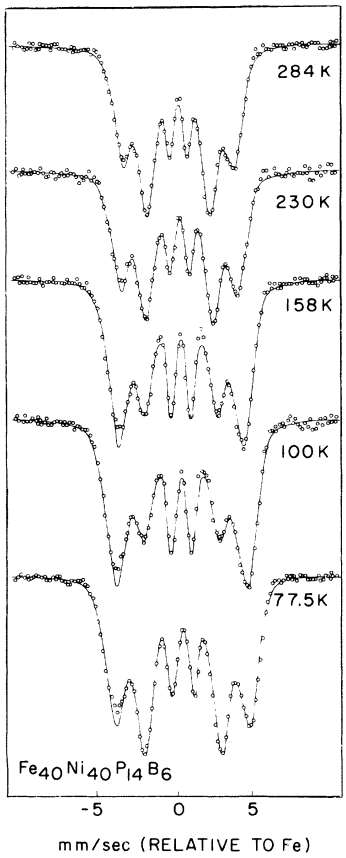

FIG. 2. Mössbauer spectra of $Fe_{40}Ni_{40}P_{14}B_6$ at low temperatures.

only if the magnetization axis for the entire ribbon is predominantly along the ribbon long edge. This conclusion is also reached by magnetic resonance measurement.[6] Since the present measurements were made in transmission geometry, the above conclusion applies to the entire thickness of the sample. However, there is evidence from domain pattern observations that on the sample surface, there are small patches of areas for which the magnetization axes may not be in the sample plane.[7]

The spectra of a sample, sandwiched by Al foils and held by thin layers of vacuum grease, at low temperatures with the γ ray perpendicular to the sample plane are shown in Fig. 2. Surprisingly, the No. 2 and 5 peaks show much lower intensities in the temperature range of 70 K $\lesssim T \lesssim$ 200 K, as previously reported.[8,9] The average magnetization axis, which is in the sample plane at 300 K, has a component perpendicular to the sample in this temperature range. It is well known that the local anisotropy of an "as-prepared" metallic glassy sample is mainly determined by the strain patterns "frozen in" during the rapid quenching process. However, it is difficult to attribute the unusual behavior at low temperatures to strain in the sample, since it would require a temperature dependence of strain which would generate out-of-plane moments only in the temperature range of 70–200 K. Experimental investigation by Egami *et al.*[10] indicated that the bulk magnetic properties of a number of glassy ferromagnets, including the present alloy, are susceptible to *external* stresses applied to the sample. This led us to suspect that the unusual behavior at low temperatures may be caused by the hardened vacuum grease, which holds the ribbons in place. Indeed, measurements of a sample covered with no vacuum grease, showed essentially in-plane magnetization at low temperatures with *no* anomaly. An "as prepared" sample at 300 K, covered with room-temperature-cured hardened epoxy, again showed a considerable amount of out-of-plane magnetization. Therefore, the "as prepared" samples of $Fe_{40}Ni_{40}P_{14}B_6$ have magnetization mainly in the ribbon plane at all temperatures. The magnetization axis is highly

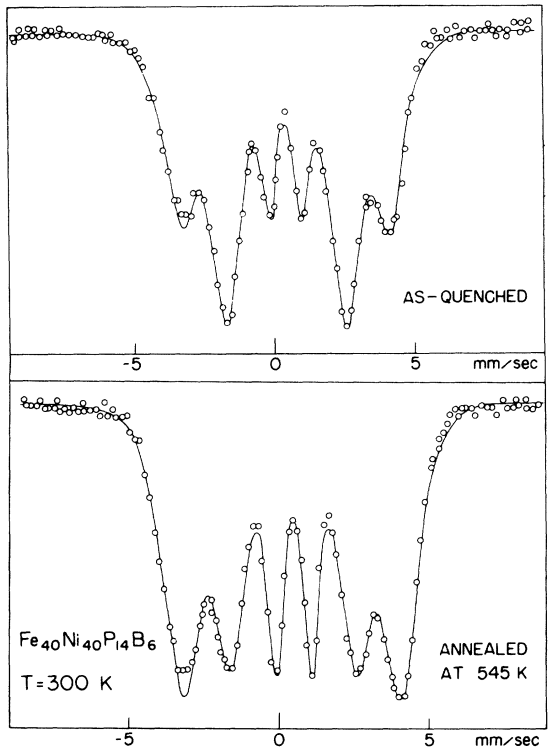

FIG. 3. Mössbauer spectra of $Fe_{40}Ni_{40}P_{14}B_6$ at 300 K for the as-quenched sample and the sample after annealing at 545 K for 2 days.

susceptible to external stresses, such as those generated by the hardened vacuum grease at low temperatures. Absorber preparation is of crucial importance, if information concerning the magnetization axis is sought.

The above results are pertinent to the "as prepared" samples, that is, samples which have not been treated with high-temperature annealing. We have also heated one sample to 545 K, which is above the Curie temperature, for two days in vacuum of 10^{-5} Torr. After the annealing, for the annealed sample at 300 K, the magnetization axis was found to have been substantially altered to more random directions, as shown in Fig. 3. This is expected, since high-temperature annealing, among other purposes, serves as a stress-release process.

It should be particularly emphasized that the above-mentioned directional change of the magnetization axis only affects the relative intensities of the spectral lines. The line positions, the total splitting and the value of $H_{\text{eff}}(T)$ are *not* altered. This is clearly illustrated in Fig. 3.

C. Temperature dependence of hyperfine field

Although $Fe_{40}Ni_{40}P_{14}B_6$ contains two transition-metal elements, Ni in this system is most likely to be nonmagnetic and Fe is the only magnetic constituent. This is shown by the studies of $(Fe_x Ni_{1-x})_{80}P_{14}B_6$. By progressively reducing the Fe content, the magnetic ordering temperature T_C is found to decrease towards $T = 0$ K.[11,12] Similar behavior has been observed in[13] $(Fe_x Ni_{1-x})_{80}P_{10}B_{10}$ and $(Fe_x Ni_{1-x})_{75}P_{16}B_6Al_3$.[14] Therefore, although the magnetic moment per transition-metal atom in $Fe_{40}Ni_{40}P_{14}B_6$ is about $1.14\mu_B$,[15] which is considerably smaller than the value of about $2\mu_B$ for the Fe-rich system, the actual Fe moment is probably close to $2\mu_B$.

Typical Mössbauer spectra of $Fe_{40}Ni_{40}P_{14}B_6$ at low and high temperatures are shown in Figs. 2 and 4. The measured reduced hyperfine fields of glassy $Fe_{40}Ni_{40}P_{14}B_6$ and crystalline Fe are shown in Fig. 5. The difference between glassy and crystalline ferromagnets is obviously great in that, the curve for the glassy ferromagnet decreases with temperatures

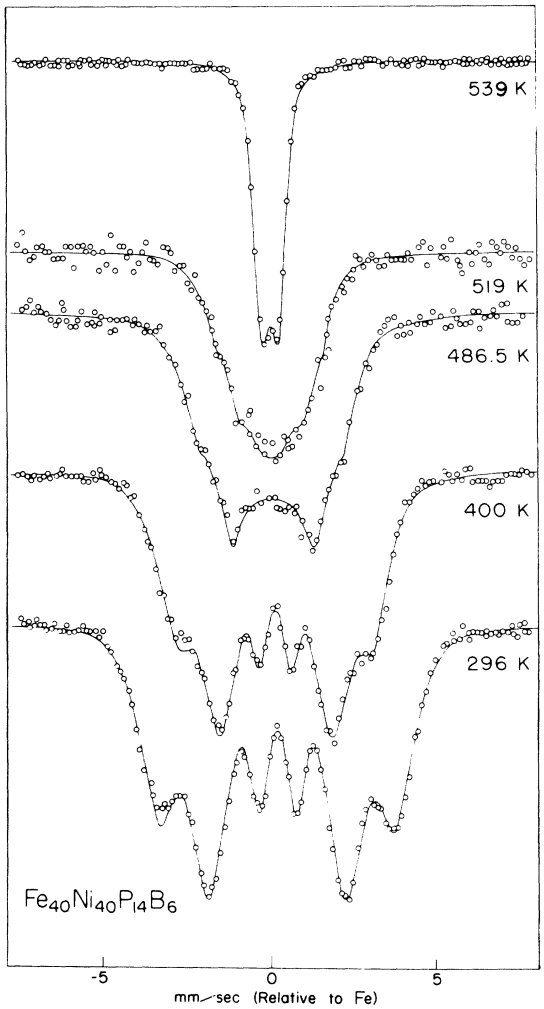

FIG. 4. Mössbauer spectra of $Fe_{40}Ni_{40}P_{14}B_6$ at $296 \leq T \leq 539$ K.

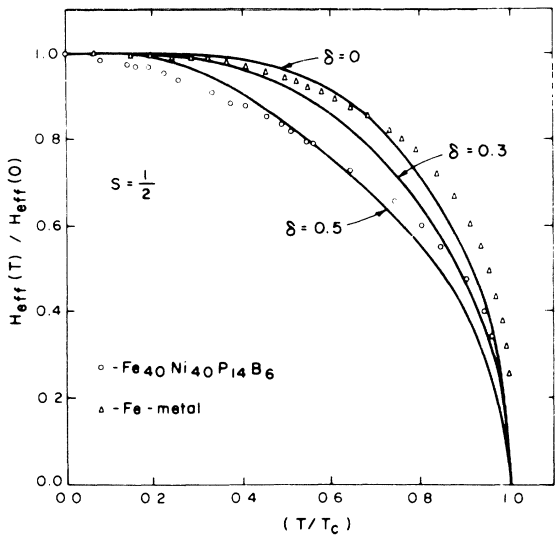

FIG. 5. Reduced hyperfine field vs reduced temperature of $Fe_{40}Ni_{40}P_{14}B_6$ (circles) and Fe metal (triangles). The solids curves are results obtained from Eq. (1).

much more rapidly. The reduced curvature seems to be a general feature of noncrystalline ferromagnets.[16]

Magnetization and Mössbauer spectroscopy measurements in a number of glassy ferromagnets, including the present sample, suggest that, to a very good approximation, the measured hyperfine field $H_{\text{eff}}(T)$ and the magnetization $M(T)$ are proportional.[17] The temperature dependence of the reduced hyperfine field then, as shown in Fig. 5, reflects the temperature dependence of the reduced magnetization.

The lower magnetization curve for the glassy ferromagnets is due to a distribution of exchange interactions because of the disordered structure. A number of theoretical calculations of the magnetization of noncrystalline ferromagnet have taken into account, through various models, a distribution of exchange interactions.[18-20] Many of these calculations have used the molecular-field approximation.[18] Of these, the results obtained by Handrich have a simple analytical form. Handrich considered a random fluctuation of the exchange constants in the Heisenberg interaction and used the molecular-field approximation. The reduced magnetization for a glassy ferromagnet has the form

$$\sigma = M(T)/M(0) = \tfrac{1}{2}\{B_S[(1+\delta)x] + B_S[(1-\delta)x]\}, \quad (1)$$

with

$$x = 3S(S+1)T_C\sigma/T$$

where B_S is the Brillouin function for spin S, T_C is the Curie temperature, and $0 < \delta < 1$ is a measure of the fluctuation of the exchange interactions. Equation (1) retains the well-known form for crystalline ferromagnets by setting $\delta = 0$, i.e.,

$$\sigma = B_S(x) . \quad (2)$$

Eq. (1) indeed predicts a lower magnetization curve than does Eq. (2). The amount of deviation depends on the value of δ as shown in Fig. 5. One therefore can compare the experimental data with the calculated results in order to estimate the value of δ. For the present case, a value of $\delta \simeq 0.5$ can be assigned as a reasonable estimate.

Although Eq. (1) predicts a lower curve for glassy ferromagnet, in qualitative agreement with the experimental results, quantitatively it is still inadequate. As shown in Fig. 5, none of the curves calculated from Eq. (1) fits the experimental results for an extended temperature range. Similarly, the $\delta = 0$ curve for a crystalline ferromagnet does not agree closely with the results for crystalline Fe or Ni either. Generally, the results predicted by Eq. (1) are higher than the experimental results at low temperatures, and lower at high temperatures. These discrepancies are due to the deficiencies of the molecular-field approximation. In particular, Eq. (1) and Eq. (2) predict for σ, an exponential behavior at low temperatures and a $(T - T_C)^{1/2}$ behavior at T close to T_C. Both of these predictions are contrary to experiments as well as more precise theoretical calculations. Nevertheless, it should be pointed out that the theories by Handrich and others clearly indicate that the observed lower curve for glassy ferromagnets can be explained by taking into account a distribution of exchange interactions.

D. Spin waves

It is well known that the decrease of magnetization $M(T)$ of a crystalline ferromagnet at low temperatures has a temperature dependence of[21]

$$M(T)/M(0) = \sigma = 1 - BT^{3/2} \cdots \quad (3)$$

or

$$\Delta M(T)/M(T) = [M(0) - M(T)]/M(0) = BT^{3/2} + \cdots \quad (4)$$

instead of the exponential dependence predicted by the molecular-field approximation. This is due to the excitations of the long-wavelength spin waves. This temperature dependence has been observed in many crystalline ferromagnets.[21] In particular, for crystalline Fe and Ni, the values of $B = (3.4 \pm 0.2) \times 10^{-6}\ \text{K}^{-3/2}$ and $B = (7.5 \pm 0.2) \times 10^{-6}\ \text{K}^{-3/2}$, respectively, have been determined.[22] The difference in the values of B for Fe and Ni is largely due to the different values of the magnetic order-

TABLE I. Sample compositions, Curie temperature T_C, and coefficients B and $B_{3/2}$ for glassy $Fe_{40}Ni_{40}P_{14}B_6$ and crystalline Fe and Ni.

	T_C (K)	B (10^{-6} $K^{-3/2}$)	$B_{3/2}$	Ref.
$Fe_{40}Ni_{40}P_{14}B_6$	537	38 ± 2	0.47 ± 0.007	This work
Crystalline Fe	1043	3.4 ± 0.2	0.114 ± 0.007	22
Crystalline Ni	627	7.5 ± 0.2	0.117 ± 0.003	22

ing temperature T_C as shown in Table I. If one instead rewrites Eq. (4) as

$$\Delta M(T)/M(0) = B_{3/2}(T/T_C)^{3/2} + \cdots, \quad (5)$$

the values of $B_{3/2}$ for both Fe and Ni are almost identical (Table I). Because these values of $B_{3/2}$ are small, at low temperatures the decrease of $M(T)$ or $H_{\text{eff}}(T)$ is also small.

For $Fe_{40}Ni_{40}P_{14}B_6$ and several other glassy ferromagnets,[23-25] the decrease of the hyperfine field $H_{\text{eff}}(T)$ at low temperatures is also characterized by the $T^{3/2}$ dependence. This is shown in Fig. 6, in which the plot of fractional change of $H_{\text{eff}}(T)$ vs $(T/T_C)^{3/2}$ clearly shows a straight line. However, the values of $B = (38 \pm 2) \times 10^{-6}$ $K^{3/2}$ and $B_{3/2} = 0.47 \pm 0.03$ for $Fe_{40}Ni_{40}P_{14}B_6$ are many times *larger* than those of Fe and Ni (Table I). In Fig. 6, the dashed line (for Fe and Ni) and the solid line illustrate this large difference. Furthermore, the temperature range in which the $T^{3/2}$ term dominates is large (up to about 0.5 T_C),[17,23] whereas in crystalline Fe and Ni, the $T^{3/2}$ term holds only at much smaller temperature ranges of about 0.15 T_C.[22]

For a crystalline ferromagnet, the crystal momenta are quantized. The quadratic spin-wave dispersion relation

$$E(k) = Dk^2 + \cdots \quad (6)$$

at small wave vector k and Eq. (3) can be formally shown.[21] The quantity D in Eq. (6) is commonly called the spin-wave stiffness constant. In a glassy ferromagnet, with the absence of translational invariance, crystal momentum is no longer a good quantum number. On the other hand, the existence of spin waves should be no more surprising than the existence of sound waves in noncrystalline solids. Herring and Kittel have shown that spin waves can exist in a continuous ferromagnetic medium; that is for long-wavelength spin waves, the detailed noncrystalline arrangement of atoms would not be important.[26]

Strong experimental evidence of spin waves in glassy ferromagnets, is provided by neutron diffraction measurements.[27-29] Although glassy samples present some experimental difficulties (e.g., small momentum transfer due to the absence of a lattice), data obtained by various studies clearly show well-defined spin waves and the quadratic dispersion relation. Therefore, the observed $T^{3/2}$ dependence from the hyperfine field measurements in the present as well as other glassy samples is due to the excitations of spin waves in a noncrystalline ferromagnet.

However, the anomalously large values of B or $B_{3/2}$ for glassy ferromagnets are not explained at present. It appears that this is one of the significant differences between crystalline and glassy

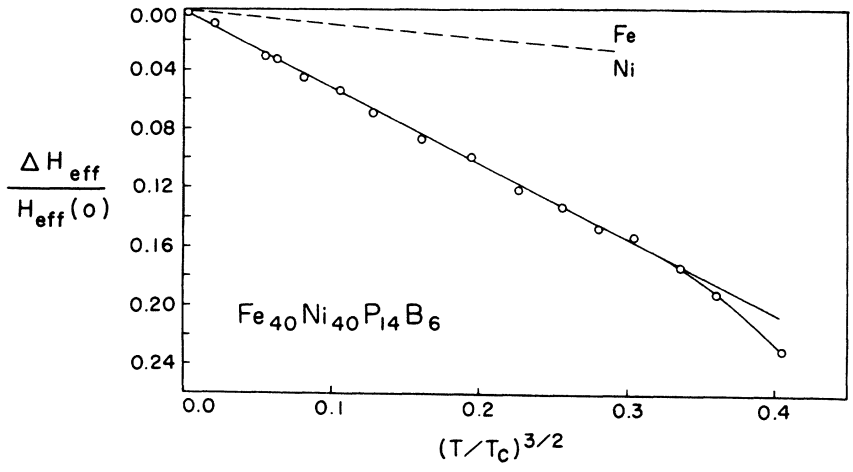

FIG. 6. Fractional change of hyperfine field vs $(T/T_C)^{3/2}$ for $Fe_{40}Ni_{40}P_{14}B_6$. The dashed line indicates the corresponding change for crystalline Fe and Ni.

ferromagnets. Another puzzling aspect for glassy ferromagnets is the discrepancy in the spin-wave stiffness constant D. In several glassy ferromagnetic systems, neutron diffraction studies[27-29] indicate a stiffer constant than that obtained by Mössbauer spectroscopy,[17,23] magnetization,[4,16,30] and ferromagnetic resonance measurements.[31]

E. At $T \simeq T_C$

Because the exchange interaction between magnetic spins in a glassy magnetic solid is no longer unique due to the disordered atomic arrangement, some questions of fundamental interest concerning the magnetic phase transition arise. Aspects of particular interest are whether the transition is a sharp second order transition or a "smeared" transition; and in the case of sharp transition, whether the critical behavior is different from that of crystalline magnetic systems. However, not every glassy magnetic system can be investigated in the temperature range close to the critical temperature T_C. As mentioned earlier, the glassy state is metastable only at temperatures lower than the crystallization temperature T_{cr}. In systems for which T_{cr} is lower than T_C, T_C can never be experimentally reached without destroying the glassy state. In many cases, crystallization sets in after prolonged heating at temperatures below T_{cr} such as in $Fe_{80}B_{20}$,[24] $Fe_{80}P_{16}B_1C_3$,[32] and others.

For the present sample of glassy $Fe_{40}Ni_{40}P_{14}B_6$, T_{cr} is over 150 K above T_C, so that prolonged measurements at T close to T_C for a period of a few weeks did not induce crystallization of the sample. The magnetic ordering temperature $T_C = 537$ K has been found to be sharply defined to be within 2 K and there is no sign of a "smeared" transition. This should be contrasted with amorphous $TbFe_2$ for example, in which the "smeared" transition region is as large as 0.1 T_C.[33] At temperatures close to T_C, the hyperfine field of the present samples varies as a power law of

$$H_{\text{eff}}(T)/H_{\text{eff}}(0) = D(1 - T/T_C)^{\beta} \tag{7}$$

as shown in Fig. 7 with critical parameters $\beta = 0.32 \pm 0.05$ and $D = 1.03 \pm 0.03$. These values are not very much different from those of crystalline ferromagnets. Because the inherent linewidths are broad due to the hyperfine field distribution, spectral resolution is poorer than that obtained from a crystalline solid with one magnetic site. Resolution can be obtained only for spectra taken at reduced temperature $1 - T/T_C \gtrsim 0.01$.

F. Quadrupole interaction and isomer shift

At temperatures higher than $T_C = 537$ K, glassy $Fe_{40}Ni_{40}P_{14}B_6$ is paramagnetic. The resultant spectrum consists of a doublet as shown in Fig. 8. The fitted curve assumes two independent Lorentzians. As mentioned earlier, the doublet spectrum is expected from the noncrystalline nature of the sample, in which the Fe site symmetries are in general noncubic. For the same reason, quadrupole spectra are expected for all glassy magnetic solids in their paramagnetic states.[34]

Since the local symmetry axes vary spatially throughout the sample, the ^{57}Fe quadrupole spectrum should be a symmetric doublet of equal intensities. This is *not* observed in the present samples and many other glassy magnetic systems at $T > T_C$. Instead, as shown in Fig. 8, one observes two peaks of slightly different intensities but with approximately the same spectral areas. The possibility of a Goldanskii-Karayagin effect[35] can be

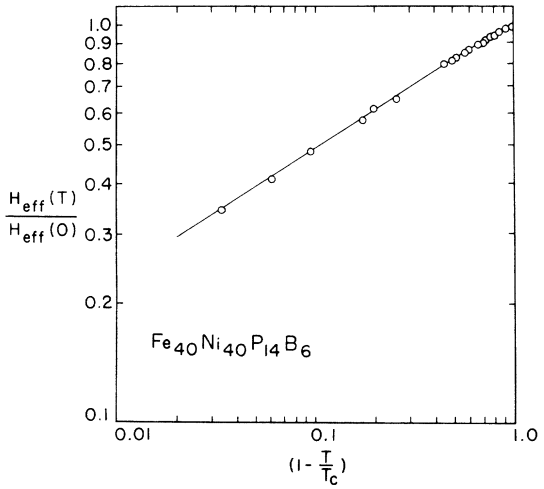

FIG. 7. $\log\{H_{\text{eff}}(T)/H_{\text{eff}}(0)$ vs $\log(1 - T/T_C)$ for $Fe_{40}Ni_{40}P_{14}B_6$.

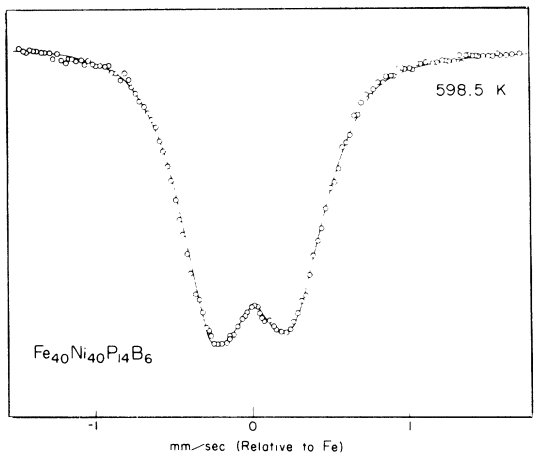

FIG. 8. Mössbauer spectra of glassy $Fe_{40}Ni_{40}P_{14}B_6$ at 598.5 K.

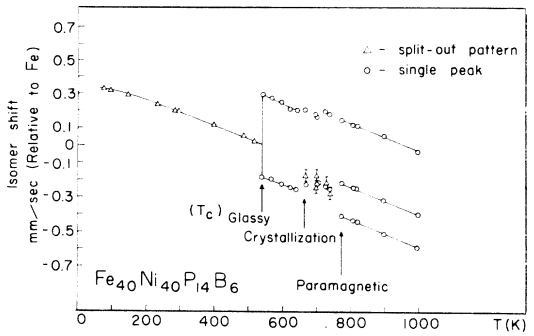

FIG. 9. Temperature dependences of isomer shift of $Fe_{40}Ni_{40}P_{14}B_6$. (T_C) glassy is the Curie temperature of the glassy state; "crystallization" indicates the temperature at which crystalline phases begin to appear; "paramagnetic" indicates the temperature above which the crystallized sample of $Fe_{40}Ni_{40}P_{14}B_6$ is paramagnetic.

ruled out both from the structural considerations and from the fact that the asymmetry is independent of temperature.[34] The asymmetrical doublet is probably due to the existence of distributions of isomer shifts and quadrupole splittings. It follows then the electronic states of all Fe atoms are not identical. The measured isomer shift (centroid of the doublet) and quadrupole splitting (separation of the two peaks) are therefore mean values.

The random atomic arrangements in glassy magnetic solids might imply that the electric field gradients at various Fe sites have a wide range of values. A collective measurement of all these different quadrupole interactions might lead to a structureless "washed-out" spectrum. The well-defined doublet spectra observed indicate that this is not the case. The actual distribution of the quadrupole interaction must be rather narrow. Theoretical calculations by Cochrane *et al.* have also suggested this feature.[36]

The temperature dependence of the isomer shift is shown in Fig. 9. For the magnetic hyperfine pattern, the centroid of the six-line pattern is taken as the isomer shift. For the paramagnetic spectra, the actual peak positions are shown. As shown in Fig. 9, the value of the isomer shift decreases as temperature is increased. This dependence can be adequately described by the second-order Doppler effect, shown by the solid lines in Fig. 9. Between $T = 537$ K and 670 K, the quadrupole splitting of 0.46 mm/s is essentially temperature independent.

G. Glassy to crystalline transition

There is no qualitative change of the quadrupole spectrum from 537 K to about 670 K as shown in Fig. 10. However, at about 670 K, a spontaneous change of the spectrum occurs: a magnetic hyperfine pattern, although not well resolved, appears (the 672.5-K spectrum in Fig. 10) and the doublet spectrum in the center of the same spectrum has a slightly different splitting (Fig. 9) and intensity ratio (Fig. 10) than those of the 646-K spectrum. This is because the glassy state has been irreversibly destroyed, and 670 K is the lower limit of the crystallization temperature T_{cr}. The split-out pattern in the 672.5-K spectrum is due to the crystalline phase with magnetic ordering temperature higher than 672.5 K. The doublet spectrum in the center of the 672.5-K spectrum is not due to glassy $Fe_{40}Ni_{40}P_{14}B_6$ in the paramagnetic state, but rather, it is due to the crystalline phases with magnetic ordering temperatures lower than 672.5 K. Therefore from this spectrum alone, one concludes that there are at least two crystalline phases

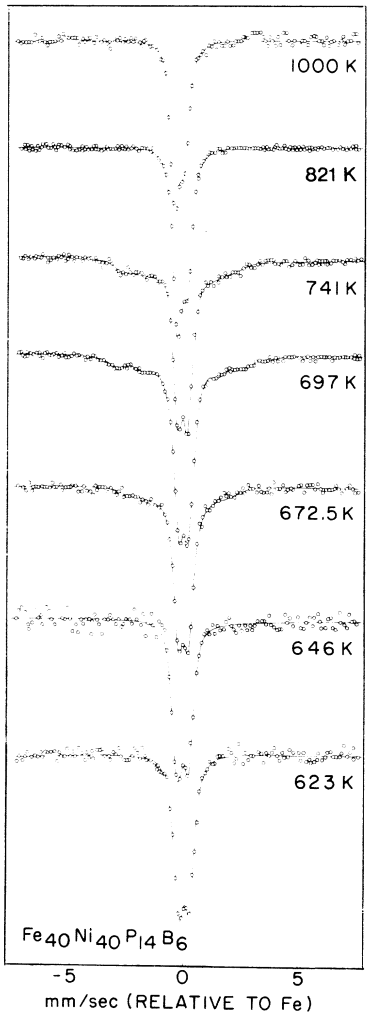

FIG. 10. Mössbauer spectra of $Fe_{40}Ni_{40}P_{14}B_6$ at high temperatures, showing the crystallization behavior.

in the crystallized sample of $Fe_{40}Ni_{40}P_{14}B_6$.

The reason that 670 K is indicated to be the lower limit of the crystalization temperature T_{cr} is that T_{cr} is defined only for very high heating rate.[37] For lower heating rate, the crystallization temperature generally appears at a lower temperature. Prolonged heating at T less than T_{cr} will eventually induce crystallization. For this reason, we have also heated on glassy sample of $Fe_{40}Ni_{40}P_{14}B_6$ at a high heating rate of 30 K/min, and crystallization has been found to occur at a higher temperature of 700 K. Higher heating rate than 30 K/min has resulted in no appreciable change of the temperature at which crystallization occurs. We, therefore, assigned $T_{cr} = 700$ K as the crystallization temperature of glassy $Fe_{40}Ni_{40}P_{14}B_6$.

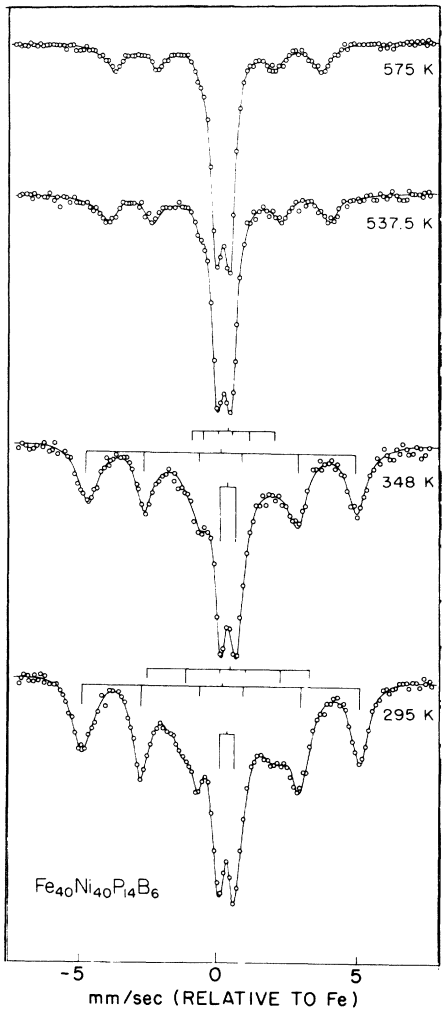

FIG. 11. Mössbauer spectra of the crystallized sample of $Fe_{40}Ni_{40}P_{14}B_6$. The magnetic spectra with the larger hyperfine splitting are due to Fe-Ni alloy. The spectra with smaller hyperfine splitting in the 348- and 295-K spectra are due to $(Fe\text{-}Ni)_{30}P_7B_3$.

H. Crystalline phases

As shown in Fig. 10, above 750 K the crystallized sample is paramagnetic with the resultant spectra consisting of three peaks. The peak positions of these peaks are shown in Fig. 9 up to 1000 K.

The fact that above 750 K there is no magnetic ordering indicates that there is no crystalline phases with ordering temperature higher than 750 K. In particular, there is no detectable amount of α-Fe, a common phase of Fe-containing glassy solids after crystallization because its magnetic ordering temperature is 1043 K.

As the temperature is lowered from 1000 K, one six-line pattern appears at 750 K, as shown by the 575 and 537.5 K spectra in Fig. 11. A second six-line pattern appears at 425 K as shown by the 348 and 295 K spectra in Fig. 11. Therefore, there are at least two crystalline phases with magnetic ordering temperatures of 750 K and 425 K. These crystalline phases must contain the available elements in the original glassy sample. X-ray diffraction measurements[38] on the crystallized sample indicate two crystalline phases of fcc $Fe_{55}Ni_{45}$ ($T_C = 750$ K) and tetragonal $(Fe_{0.58}Ni_{0.42})_{30}P_7B_3$ ($T_C = 425$ K). The Fe sites in the latter are noncubic so there is a nonzero quadrupole interaction. This is indeed observed in both the paramagnetic and the magnetic spectra as shown in Fig. 11.

However, as shown by the 295-K spectrum in Fig. 11, in addition to the two sets of six-line patterns, there is still a doublet in the central portion of the spectrum. This indicates perhaps a third crystalline phase which order below 295 K. However, as shown in Fig. 12, the doublet gradually disappears at about 200 K with no sharply defined ordering temperature. This can be better shown by the constant Doppler velocity thermoscan measurement as shown in Fig. 13. At the onset of the magnetic ordering of each crystalline phase, the count rate measured near the centroid of the spectrum also reflects these changes. The magnetic ordering temperatures of 750 K and 425 K can be clearly detected. However, at 425 K and below, there is a general increase, with no sharp increase in count rate, indicative of well-defined magnetic ordering points. There are two possibilities for this somewhat unusual results:

(i) There may be crystalline phases with ordering temperatures spread over from 200 to 425 K, since the relative Fe and Ni contents in $(Fe\text{-}Ni)_{30}P_7B_3$ could conceivably be varied, resulting in a range of ordering temperatures;

(ii) Superparamagnetic behavior of only one cry-

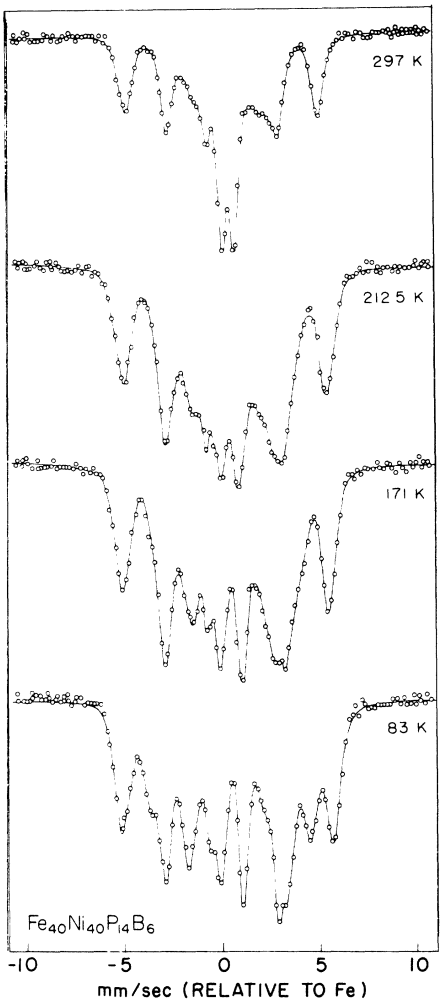

FIG. 12. Mössbauer spectra of the crystallized sample of $Fe_{40}Ni_{40}P_{14}B_6$ at 83 K $\leq T \leq$ 297 K. The 83-K spectrum can be well-described by two magnetic hyperfine patterns.

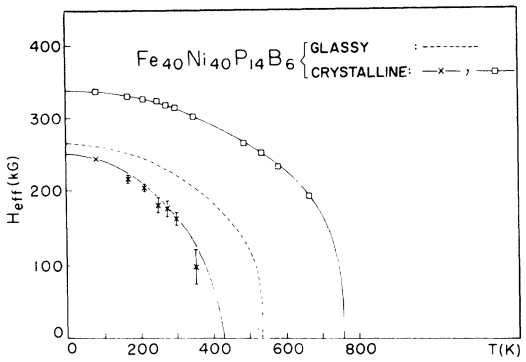

FIG. 14. Temperature dependences of the hyperfine field $H_{eff}(T)$ of $Fe_{40}Ni_{40}P_{14}B_6$ in the glassy state (dashed curve) and the two crystalline phases after crystallization.

stalline phase with $T_C = 425$ K, since the grain size of the crystalline phases are generally small (a few hundred Å).[37] These two possibilities have not been distinguished from the experimental results, although the spectrum measured at 83 K, as shown in Fig. 12, can be well described by two sets of six-line patterns.

From the area ratio of the spectra taken at 83 K and below, approximately $\frac{1}{3}$ of the Fe atoms are contained in the $Fe_{55}Ni_{45}$ phase and $\frac{2}{3}$ are contained $(Fe-Ni)_{30}P_7B_3$ phase. In order to check whether the crystalline phases formed depend on the heating rate with which the glassy sample was crystallized, we have also measured one crystallized sample which was crystallized under a high heating rate of over 30 K/min. The same two crystalline phases were also found except that the area ratio of the two crystalline phases is considerably different from the case mentioned above.

The temperature dependence of the hyperfine

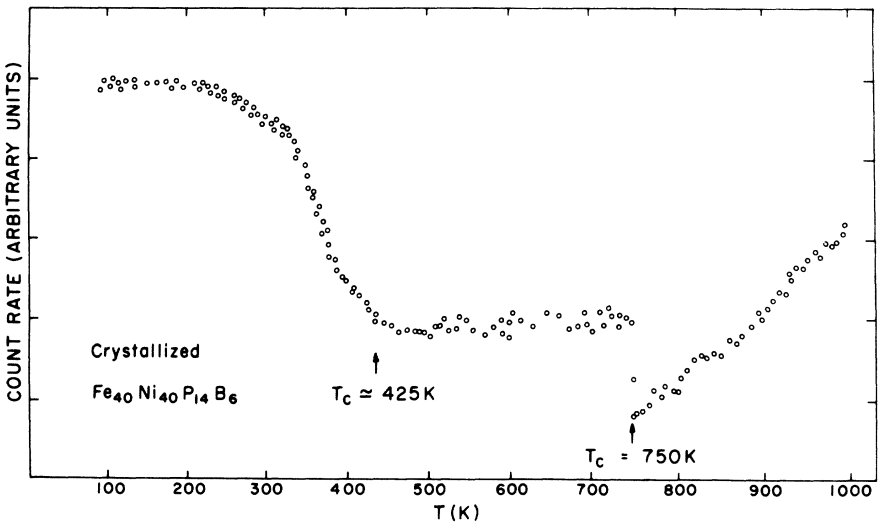

FIG. 13. Count rate measured near the centroid of the spectrum of the crystallized sample of $Fe_{40}Ni_{40}P_{14}B_6$ as a function of temperatures. The crystalline phases with two distinct Curie temperatures of 750 and 425 K can be easily detected.

fields of the two crystalline phases are shown in Fig. 14. The dashed curve indicates the behavior of the glassy state. One notes that both the values of $H_{\text{eff}}(0)$ and T_C of the glassy state are between those of the two crystalline phases.

IV. CONCLUSIONS

Metallic glassy ferromagnet $Fe_{40}Ni_{40}P_{14}B_6$ has been studied from 4.2 to 1000 K by Mössbauer spectroscopy. In the glassy state, the "as-prepared" sample has a magnetization axis in the ribbon plane. The magnetization direction is highly susceptible to external stresses. The anomalous change of magnetization axis at low temperatures as reported earlier is caused by stress produced by hardening of the vacuum grease mounting. The reduced hyperfine field $H_{\text{eff}}(T)/H_{\text{eff}}(0)$ decreases with the reduced temperature T/T_C much more rapidly than that of a crystalline ferromagnet as a result of a distribution of exchange interactions. Theoretical calculations using the molecular-field approximation with the inclusion of a distribution of exchange interactions can only qualitatively but not quantitatively describe the observed results. At low temperature, $H_{\text{eff}}(T)/H_{\text{eff}}(0)$ has a temperature dependence of $1 - B_{3/2}(T/T_C)^{3/2} \cdots$ in a large temperature range due to long-wavelength spin-wave excitations. The value of the coefficient $B_{3/2} = 0.47$ is four times larger than those of crystalline Fe and Ni.

The magnetic ordering temperature $T_C = 537$ K is found to be sharply defined to at least $0.01\ T_C$. At temperatures below T_C, the reduced hyperfine field varies as $D(1 - T/T_C)^{\beta}$ with $D = 1.03 \pm 0.03$ and $\beta = 0.32 \pm 0.05$.

At $T > 537$ K, the glassy state is paramagnetic. Well-defined quadrupole spectra consisting of two peaks are observed. However, the observed asymmetrical doublets suggest that the electronic states of Fe in the sample are not identical. In the limited temperature range of $537\ \text{K} \leq T \leq 670$ K, the quadrupole splitting is essentially temperature independent.

The crystallization temperature $T_{cr} = 700$ K has been determined under high heating rate of 30 K/min. For a much lower heating rate, the crystallization process has been found to occur at 670 K. There are two major crystalline phases in the crystallized sample: $Fe_{55}Ni_{45}$ ($T_C = 750$ K) and $(Fe_{0.58}Ni_{0.42})_{30}P_7B_3$ ($T_C = 425$ K).

---

†Supported by NSF.

[1]See, e.g., *Amorphous Magnetism*, edited by H. O. Hooper and A. M. de Graff (Plenum, New York, 1972); *Proceedings of the Second International Symposium on Amorphous Magnetism*, edited by R. A. Levy and R. Hasegawa (Plenum, New York, 1977).
[2]G. S. Cargill, Solid State Phys. 30, 27 (1974).
[3]Registered trademark of Allied Chemical Corp.
[4]C. C. Tsuei and H. Lilienthal, Phys. Rev. B 13, 4899 (1976).
[5]See, e.g. G. Wertheim, *Mössbauer Effect: Principles and Its Applications* (Academic, New York, 1964).
[6]R. Hasegawa, AIP Conf. Proc. 29, 216 (1975).
[7]J. J. Becker, AIP Conf. Proc. 29, 204 (1975).
[8]C. L. Chien and R. Hasegawa, AIP Conf. Proc. 29, 214 (1975).
[9]C. L. Chien and R. Hasegawa, J. Appl. Phys. 47, 2234 (1976).
[10]T. Egami, P. J. Flaners, and C. D. Graham, Appl. Phys. Lett. 26, 128 (1975); T. Egami, P. J. Flanders, and C. D. Graham, AIP Conf. Proc. 24, 697 (1975).
[11]J. J. Becker, F. E. Luborsky, and J. L. Walter, IEEE Trans. Magn. 13, 988 (1977).
[12]C. L. Chien, D. P. Musser, F. E. Luborsky, J. J. Becker and J. L. Walter, Solid State Commun. (to be published).
[13]T. Mizoguchi, K. Yamauchi, and H. Miyajina in *Amorphous Magnetism*, edited by H. O. Hooper and A. M. de Graff (Plenum, New York, 1972).
[14]R. C. Sherwood, E. M. Gyorgy, H. S. Chen, S. D. Ferris, G. Norman, and H. J. Leamy, AIP Conf. Proc. 24, 745 (1975).
[15]R. Hasegawa, R. O. O'Handley, L. E. Tanner, R. Ray, and S. Kavesh, Appl. Phys. Lett. 29, 219 (1976).
[16]T. Mizoguchi, AIP Conf. Proc. 34, 286 (1976).
[17]C. L. Chien and R. Hasegawa, Phys. Rev. B, in press.
[18]K. Handrich, Phys. Status Solidi 32, K55 (1969).
[19]S. Kobe, Phys. Status Solidi 41, K13 (1970).
[20]S. Kobe and K. Handrich, Fiz. Tverd. Tela 13, 887 (1971), [Sov. Phys.-Solid State 13, 734 (1971)].
[21]See, e.g., F. Keffer, in *Handbuch der Physik*, edited by S. Flügg (Springer, Berlin 1966), Vol. XVIII/2.
[22]B. E. Argyle, S. H. Charap, and E. W. Pugh, Phys. Rev. 132, 2051 (1963).
[23]C. L. Chien and R. Hasegawa, AIP Conf. Proc. 31, 366 (1976).
[24]C. L. Chien and R. Hasegawa, in *Proceedings of the Second International Symposium on Amorphous Magnetism* (Plenum, New York, 1977).
[25]C. L. Chien and R. Haseagwa, J. Phys. (Paris) Colloq. 6, 759 (1976).
[26]C. Herring and C. Kittel, Phys. Rev. 81, 869 (1951).
[27]H. A. Mook, N. Wakabayashi and D. Pan, Phys. Rev. Lett. 34, 104 (1975).
[28]J. D. Axe, P. Passell and C. C. Tsuei, AIP Conf. Proc. 24, 119 (1975).
[29]J. W. Lynn, G. Shirane, R. J. Birgeneau, and H. S. Chen, AIP Conf. Proc. 34, 313 (1976).
[30]R. W. Cochrane and G. S. Cargill, Phys. Rev. Lett. 32, 476 (1974).
[31]J. R. McColl, D. Murphy, G. S. Cargill, and T. Mizoguchi, AIP Conf. Proc. 29, 172 (1976).

[32]C. L. Chien and R. Hasegawa, IEEE Trans. Magn. 12, 951 (1976).
[33]S. J. Pickart, J. J. Rhyne and H. A. Alperin, Phys. Rev. Lett. 33, 424 (1974).
[34]C. L. Chien, J. Hyperfine Interactions (to be published).
[35]V. I. Goldanskii and E. F. Markov, in *Chemical Applications of Mössbauer Spectroscopy*, edited by V. I. Goldanskii and R. H. Herber (Academic, New York, 1968), p. 103.
[36]R. W. Cochrane, R. Harris, M. Plischke, D. Zobin, and M. J. Zukermann, Phys. Rev. B 12, 1969 (1975).
[37]P. K. Rastogi and P. Duwez, J. Non-Cryst. Solids 5, 1 (1970).
[38]R. Hasegawa and R. C. O'Handley, *Proceedings of the Second International Conference on Rapidly Quenched Metal* (MIT, Cambridge), p. 459.